EXPERIMENTAL ANALYSIS ON FRICTION MATERIALS FOR SUPPLEMENTAL DAMPING DEVICES

M. Latour, V. Piluso & G. Rizzano
University of Salerno
Civil Engineering Department
Salerno, Italy
mlatour@unisa.it, v.piluso@unisa.it, g.rizzano@unisa.it

ABSTRACT

In this paper, the friction coefficient and the cyclic response of different interfaces for friction devices are investigated by means of experimental tests under displacement control. In particular, six interfaces have been tested: steel-steel, brass-steel, sprayed aluminum-steel and three different rubber based friction materials adopted, respectively, in automotive applications, electrical machines and applications requiring low wearing.

Static and kinetic friction coefficients have been evaluated and the influence of the interface pressure has been analyzed. The variation of the sliding force during the cyclic loading history has been investigated by comparing also the response coming from the use of different washers: circular flat washers and cone shaped annular disc springs.

The work is aimed at the investigation of friction materials to be applied within the connecting elements of beam-to-column joints according to the double split tee configuration with friction pads.

INTRODUCTION

Modern seismic resistant structures need to be designed in order to withstand frequent earthquakes without significant damages and to remain safe, even though a certain amount of structural damage is accepted, in case of rare seismic events. Concerning last case, as soon as the energy balance under seismic loading conditions is considered, it is clear that there are two main strategies to limit damage. The first one consists in minimizing structural damage by adding supplemental damping devices (Whittaker et al., 1990; Constantinou et al., 1998), either viscous or hysteretic. The second strategy consists in reducing the seismic input energy by means of seismic base isolation systems (Kelly, 1979; Aiken et al., 1993b).

Dealing with the first strategy, the development of supplemental damping devices started in New Zealand about 40 years ago (Kelly et al., 1972; Skinner et al., 1975; Aiken et al., 1993a; Christopoulos & Filiatrault, 2006). In particular, in the past few decades, the development of

supplemental damping systems has received a great attention of academics and engineers leading to the development of a number of dissipative devices (Soong & Spencer Jr, 2002; Cahis et al., 1997; Constantinou et al., 1998; Kobori et al., 1992; Nakashima, 1995; Skinner et al., 1975; Whittaker et al., 1989; Alonso, 1989). Many of these systems have been installed in buildings and bridges worldwide, both for seismic retrofit and for new constructions.

A wide category of supplemental dampers is based on dry friction for dissipating the earthquake input energy. In these elements, the energy is usually dissipated by means of the slippage between two surfaces in contact, which are clamped by means of the application of hydraulic pressures, electromagnetic forces or, in the simplest case, by means of high strength bolts. In particular, this last clamping method is, due to its simplicity, probably the most applied in civil engineering practice. In fact, by adopting high strength bolts, it is possible to apply a constant force on one or more surfaces in contact by simply governing the value of the tightening torque and the number and diameter of the bolts.

Friction dampers usually fall into the category of displacement activated dampers, because their sliding force is not dependent on the velocity and frequency content of the excitation. The cyclic behavior of friction dampers is usually described by means of a rigid-plastic response. Therefore, the only parameter needed by the designer is the slip force which, in turn, depends on the value of the load normal to the surfaces in contact and on the friction coefficient which is an intrinsic characteristic of the sliding interface. A great advantage of friction devices is that, they can be used to work as displacement reducers under service conditions while they can dissipate the seismic input energy under severe seismic actions.

The friction coefficient depends on different phenomena, such as adhesion, ploughing and the presence of contaminants. The modeling of these phenomena is usually studied in tribology where, in order to develop theories for predicting slip forces under static and dynamic loads, the surfaces' topography, materials' hardness, mechanical properties and the effects of interface layers are physically modeled. Conversely, in structural engineering, the properties of friction materials are typically studied by following the experimental approach which, for seismic engineering scopes is usually retained sufficient to provide the information needed for designing such devices.

In the technical literature several works are concerned with the characterization of the hysteretic behavior of sliding metallic surfaces with different superficial treatments clamped by means of high strength friction grip bolts. This case is particularly significant for civil engineering purposes, because the greatest part of friction dampers developed since the 70s' to be used for dissipative braces or links adopts this approach. One of the first devices of such type was that developed by (Pall & Marsh, 1981) to be introduced at the intersection of braces, which adopted asbestos brake

lining pads between the steel sliding surfaces. One of the simplest forms of friction damper has been proposed by (Tremblay & Stiemer, 1993) who adopted simple bolted slotted plates located at the end of a conventional bracing member. The brace-to-frame connection was designed to slip before yielding or buckling of the brace. In this device, friction is developed through the sliding of steel surfaces and, in order to maintain constant the slip load, disc spring washers were used. Another friction damper for chevron braces was proposed by (Mualla & Belev, 2002).

An issue of paramount importance for systems using bolts as preloading elements is the maintenance of the preloading level during the device lifetime. In fact, the fluctuation of the bolt preload can lead in some cases to unstable hysteresis loops, so that the amount of energy dissipated can be somewhat unpredictable. In addition, under cyclic loading conditions, the wearing of the friction interface can lead to the partial loss of bolt preloading and, therefore, to the degradation of the slip force.

Within this framework, in this paper, an experimental study on friction materials to be applied to supplemental damping devices is carried out. In particular, six different interfaces are considered: steel-steel interface, brass-steel interface, sprayed aluminum-steel interface and three interfaces adopting different types of friction rubber-based materials. All specimens are clamped by means of high strength bolts and are tested under cyclic loading conditions. The work is aimed at understanding the potentialities of the considered materials to design new friction devices to be directly applied within the connecting elements of dissipative beam-to-column joints in MR-Frames (Iannone et al., 2011; Latour & Rizzano, 2012), adopting as clamping method high strength bolts (Latour et al., 2011a).

FRICTION THEORIES

From the historical standpoint the major part of past tribology studies have been addressed to the investigation of friction properties of metals recognizing that there are two main sources of friction between sliding bodies: adhesion and ploughing. The adhesion component arises because when two surfaces are loaded against each other, asperities deform plastically leading to the formation of the so-called “cold-weld” junctions. Because of the intimate contact of these junctions, the shearing of the adhesive ties requires a certain sliding load. Regarding ploughing, it is due to the natural surfaces roughness, so that the relative movement between the surfaces in contact requires that one body has to lift over the other.

The simplest theory to mathematically explain the origin of the adhesion component is due to (Bowden & Tabor, 1950) who state that, being adhesion dependent on the shear resistance of the cold-weld junctions, it has to be proportional to the real contact area which, for metals with ideal

elastic-plastic behavior can be assumed equal to $A = N/\sigma_0$, where A is the real area of contact, σ_0 is the material penetration hardness and N is the load normal to the surfaces. The total friction force due to adhesion (F_A) can be expressed as:

$$F_A = As = \frac{N}{\sigma_0} s \quad \textbf{(1)}$$

being s the force per unit of area needed to shear cold-weld junctions.

As already stated ploughing is the friction force caused by the asperities of an hard metal penetrating in a softer metal. According to Bowden and Tabor theory, this contribution is estimated as follows:

$$F_P = nrh\sigma_0 \quad \textbf{(2)}$$

where n is the number of asperities, r is the half-width of the asperity and h is the height of the asperity. Therefore, the total sliding force (F) due to adhesion and ploughing is given by:

$$F = F_A + F_P = \frac{N}{\sigma_0} s + nrh\sigma_0 \quad \textbf{(3)}$$

The ploughing component is very important during the abrasion process but, in case of metals, it has been demonstrated that such contribution is negligible compared to adhesion. Therefore, Eq.(1) explains a very important property for metals, stating that the ratio between the frictional force and the normal applied load is a constant value which does not depend on the apparent area of contact. Practically, Bowden and Tabor theory explains two of the three postulates of the classical theory of dry friction, stating that:

- the total frictional force is independent of the apparent surface area of contact;
- the total frictional force that can be developed is proportional to the normal applied action;
- in case of slow sliding velocities, the total frictional force is independent on the sliding velocity.

The first two postulates are often known as Amontons laws, after the French engineer who presented them in 1699, while the third one, is due to Coulomb (Halling, 1978; Persson, 2000).

During slippage, the classical relationship to compute the tangential force acting at the sliding interface in the direction opposed to the motion is the well-known Coulomb friction equation $F = \mu N$, where F is the sliding force, N is the normal action and μ is the friction coefficient. The force of friction is always exerted in a direction opposed to the movement (in case of kinetic friction) or potential movement (in case of static friction). According to Eq.(1) the following relationship is obtained:

$$\mu = \frac{s_0}{\sigma_0} \quad \textbf{(4)}$$

where s_0 is the critical shear stress of the weaker material and σ_0 is the hardness of the softest material. Eq.(4) provides reasonable results for metals, but in case of rubber-based materials, such as friction pads, the coefficient of friction should be computed accounting for other three effects: the contact pressure (*P*), the sliding speed (*v*) and the temperature (*T*). Therefore, in general the coefficient of friction of a rubber based interface should be expressed as $\mu = \mu(P, v, T)$.

In case of rubber based materials, the particular structure of the material influences its frictional characteristics. In fact, rubber has a low elastic modulus and its real contact area is strongly affected by the magnitude of the normal load, because the material adapts to the shape of the surface asperities of the hardest material (Zhang, 1998). The behavior of polymeric materials deviates from the classical friction theory. In fact, tribology of polymers is influenced by the adhesive junctions, the shear resistance of the rubbing material in contact and the real contact area (Schallamach, 1958). The coefficient of friction of polymers, depending on the considered range of applied normal load and on the type of polymer, may be represented by means of constant or decreasing relationships (Shooter & Thomas, 1952; Bowers et al., 1953; Rees, 1957; Schallamach, 1952). In particular, several mathematical relationships have been proposed to model the friction coefficient of steel-rubber interfaces, by expressing μ as a function of the contact pressure (*P*) and of the material elastic modulus (*E*). Some of them are herein reported:

- (Thirion, 1948): $\frac{1}{\mu} = a + b\left(\frac{P}{E}\right)$ **(5)**

where *a* and *b* are empirical parameters to be found by means of experimental testing;

- (Schallamach, 1958): $\mu = K\left(\frac{P}{E}\right)^{-1/n}$ **(6)**

where the value of *K* and *n* have to be experimentally found;

- (Ratner & Sokolskaya, 1956): $\mu = \mu_\infty + a(P)^{-h}$ **(7)**

where μ_∞ is the value of the friction coefficient when the pressure is infinite, *a* is an experimental constant and *h* is the Shore hardness divided by 100. Finally, in case of rubber, another important deviation from the classical friction theory has to be pointed out. In fact, in case of polymeric materials, the friction force can be dependent on the sliding velocity. This behavior is due to the viscoelastic behavior of polymers. Notwithstanding, usually for many polymeric materials, contact temperature does not vary significantly during the loading process provided that the influence of velocity is negligible for a limited range (0.01-1 cm/s).

TESTED FRICTION MATERIALS

In order to investigate the frictional properties of different interfaces, a sub-assemblage constituted by a layer of friction material or metal placed between plates made of S275 steel (CEN, 2005a) has been developed (Fig.1). In order to allow the relative movement of the steel on the interposed material, one of the inner plates has been realized with slotted holes.

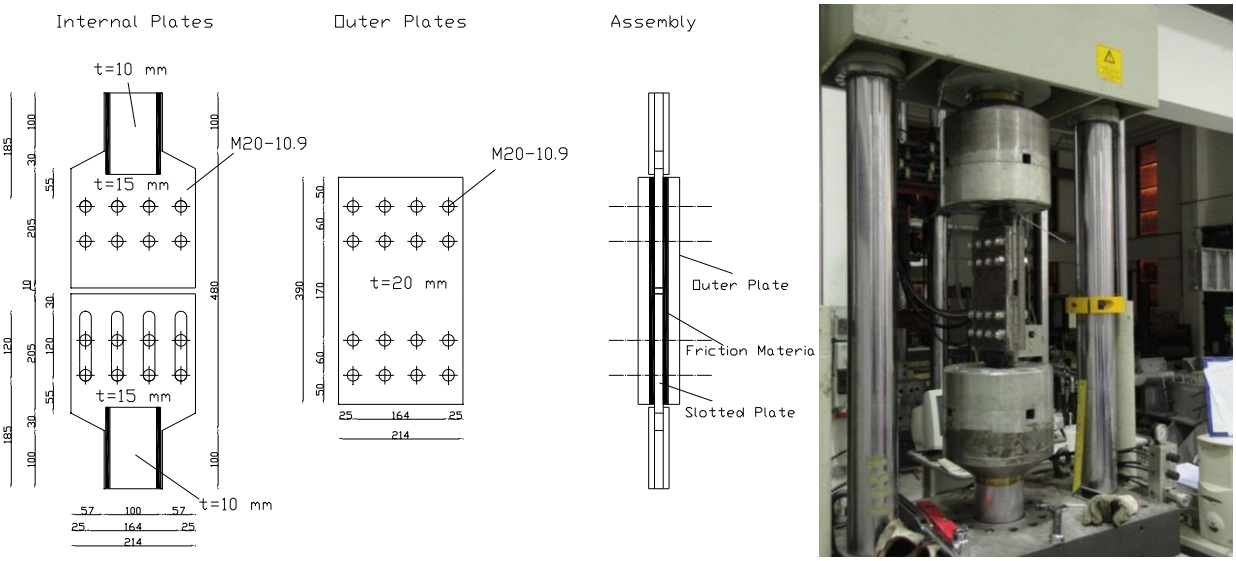

Fig. 1. Scheme of the adopted sub-assemblage and testing machine

Conversely, the other inner and the two outer plates have been realized with circular holes. The clamping force has been applied by means of preloaded M20 bolts 10.9 class (CEN, 2005b) and the holes have been drilled with a 21 mm drill bit. Aiming to evaluate the magnitude of the friction coefficient and the cyclic response, several different layouts of the sub-assemblage have been considered varying three parameters: the interface, the tightening torque, the number of tightened bolts and the type of bolt washers. In particular, the friction properties of the following six different interfaces have been investigated (Fig. 2):

- Steel on steel;
- Brass on steel;
- Sprayed Aluminum on steel;
- Friction material M0 on steel;
- Friction material M1 on steel;
- Friction material M2 on steel.

In the testing program, two different types of washers have been used. In the first part of the experimental activity, circular flat steel washers have been used, while in the second part of the campaign a packet of steel disc springs has been interposed between the bolt head and the steel plate. In addition, the experimental analysis has been carried out by varying the bolt tightening level in the range 200 Nm to 550 Nm, obtaining different values of the clamping force acting on the

sliding surface. The tightening torque has been applied in each of the loading sequences summarized in Table 1 by means of a calibrated torque wrench. Even though the use of bolt gauges allows a better calibration of the clamping force, the use of a calibrated torque wrench has been preferred, because it is commonly applied in the erection of bolted steel structures. As a consequence, the obtained testing results are referred to conditions close to those occurring on construction site.

Table 1 – Summary of the tests carried out in the experimental program

Interface	***Torque***	***Number of bolts of friction pad***	***Number of Cycles of the sequence***	***Amplitude***
Steel-Steel	*200 Nm*	4	10	+/-30 mm
	300 Nm		10	
	500 Nm		10	
Brass-Steel	*200 Nm*	8	30	+/- 15 mm
	300 Nm		20	
Sprayed Aluminum – Steel	*200 Nm*	4	10	+/- 15 mm
	300 Nm		10	
	400 Nm		10	
M0 – Steel	*300 Nm*	8	10	+/- 7.5 mm – +/- 15 mm
	400 Nm		10	
	400 Nm		10 - 10	
	500 Nm		10 - 10	
M1 – Steel	*200 Nm*	8	10	+/- 10 mm
	300 Nm		10	
	400 Nm		10	
	550 Nm		10	
M2 – Steel	*200 Nm*	8	10	+/- 15 mm
	300 Nm		10	
	400 Nm		10	

Metallic Materials

Steel S275JR

Brass

Sprayed Aluminum

Fig. 2. Texture of the Tested Materials

The main goal of the experimental program is to obtain the friction coefficients of the investigated materials, both static and kinetic, for values of the normal force varying in a range leading to sliding forces suitable for structural applications and for values of the velocity compatible with seismic engineering applications. In addition, the experimental analysis is also devoted to the evaluation of the variation of the sliding force as far as the number of cycles of the applied loading history increases. In fact, as already demonstrated by (Pall & Marsh, 1981), the response of an interface subjected to cyclic loading conditions can substantially be of two types. The first type of response provides a continuously softening behavior. In this case, the maximum sliding load is reached during the first cycle and in all the subsequent cycles a degrading behavior is exhibited. The second type of response is characterized by three phases: first an hardening response, then a steady state phase and finally a load degradation phase.

The tests have been carried out by means of a universal testing machine Schenck Hydropuls S56 (Fig. 1). The testing equipment is constituted by a hydraulic piston with loading capacity equal to +/- 630 kN, maximum stroke equal to +/- 125 mm and a self-balanced steel frame used to counteract the axial load. In order to measure the axial displacements the testing device is equipped with an LVDT, while the tension/compression loads are measured by means of a load cell. The cyclic tests have been carried out under displacement control for different amplitudes at a frequency equal to 0.25 Hz.

From the experimental results presented in the following sections, it can be recognized that the obtained displacement history does not always correspond to the imposed one. The problem is due to the ability of the testing equipment and of its electronic control system in reproducing the imposed displacement history whose accuracy reduces as far as the testing frequency increases. However, this does not constitute a problem for the interpretation of testing results, because the actually developed displacement history is accurately measured. Therefore, given the testing equipment, the testing frequency has been selected as a compromise between the opportunity to

accurately control the applied displacement history and the need to test the specimens at frequency levels comparable to those occurring under seismic actions.

EXPERIMENTAL TESTS WITH CIRCULAR FLAT WASHERS

The main goals of the experimental activity described in this paper are on one hand, the evaluation of the static and kinetic friction coefficients for different values of the normal force acting on the sliding interface and, on the other hand, the assessment of the cyclic response in order to evaluate the stability of the obtained cycles and their energy dissipation capacity. The test results reported in the following paragraphs are represented in terms of friction coefficient, which can be easily determined as:

$$\mu = \frac{F}{m\, n\, N_b} \tag{8}$$

where m is the number of surfaces in contact, n is the number of bolts, F is the sliding force and N_b is the bolt preloading force, defined starting from the knowledge of the tightening torque by means of the following expression:

$$N_b = \frac{T_b}{0.2\, d} \tag{9}$$

where T_b is the value of the tightening torque and d is the bolt nominal diameter. In this section the results of the experimental activity are reported pointing out the main features of all the tested frictional interfaces. For the sake of clarity, in the following, the materials are divided into two groups: the interfaces composed by metal plates and the interfaces composed by rubber pads sliding on steel.

Metallic Materials

Within this paper, three friction interfaces composed by different types of metal plates sliding on steel have been tested. In particular, the first series of tests has been carried out on a steel-steel interface made of S275JR structural steel (CEN, 2005a) on which three tests defined according to the loading protocol reported in Table 1 have been carried out. The results of the tests are represented in Fig. 3 in terms of μ–δ diagrams, pointing out that the cyclic behavior of the steel-steel interface is quite unstable, even though the amount of dissipated energy is significant. In particular, in the first test (1^{th}-10^{th} cycle) the specimen exhibited a very steep initial stiffness and after reaching the static sliding force began to slide with a lower force, pointing out that the static coefficient of friction is slightly greater than the dynamic one. After the first loading branch, all the subsequent cycles reached values of the maximum force greater than the initial one, showing a

significantly hardening behavior. This behavior can be due to two effects: the first one is ploughing, the second one is the steel strain-hardening. The former is related to the fact that, initially the two surfaces in contact are smooth while, after the first cycles of sliding motion, due to the wearing of the steel in the zone under the bolt heads, the number of asperities increases and the surfaces become rougher. Therefore, the increase of the number of asperities increases the magnitude of the ploughing component.

The second effect is related to the steel strain hardening which may affect the friction coefficient by varying the ratio between the steel shear strength and the steel hardness (Eq.(4)). This hardening behavior, which is quite common in case of metallic interfaces, has been also documented in a work devoted to the study of energy dampers (Grigorian et al., 1992). In the second and third loading step, i.e. from the 11^{th} to 30^{th} cycle, the response of the interface is completely different. In this case, static and dynamic sliding loads assume similar values and the maximum force experienced during the whole loading history is reached during the first cycle. In fact, it is possible to observe a continuously softening behavior which can be due to the wearing of the steel and partially to the loss of the bolt preloading. The wearing of steel is due to the high stresses acting on the interface which lead to abrasion during the motion (Fig. 4).

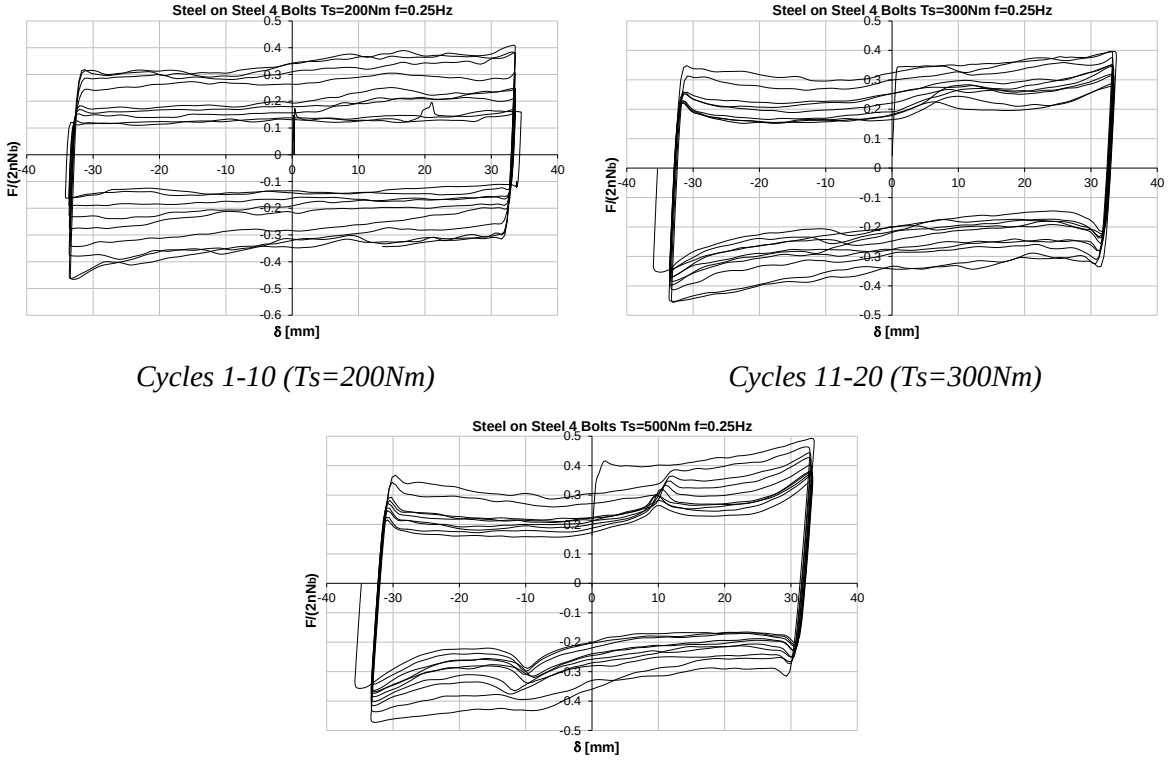

Cycles 1-10 (Ts=200Nm) *Cycles 11-20 (Ts=300Nm)*

Cycles 21-30 (Ts=500Nm)

Fig. 3. Friction Coefficient – Displacement curves of steel-steel interface

Steel S275JR *Brass* *Sprayed Aluminium*

Fig. 4. Texture of the Metallic Materials after the test

In addition, two experimental tests at different values of the applied preloading have been carried out on a steel-brass interface. Brass is an alloy of copper and zinc containing in minor part also iron and lead. The tested material is the *CuZn39Pb3*. The mechanical and chemical properties of this type of brass are reported in
Table 2.

Table 2 - Chemical Composition an mechanical properties of CuZn39Pb3 Copper Alloy (%)

Copper (Cu)	**Zinc (Zn)**	**Iron (Fe)**	**Lead (Pb)**	**Yield Strength [MPa]**	**Ultimate Tensile Strength [MPa]**	**Elongation at break [%]**	**Vickers Hardness (HV)**
55-60	40	<0.35	2-3.80	140	415	30	116

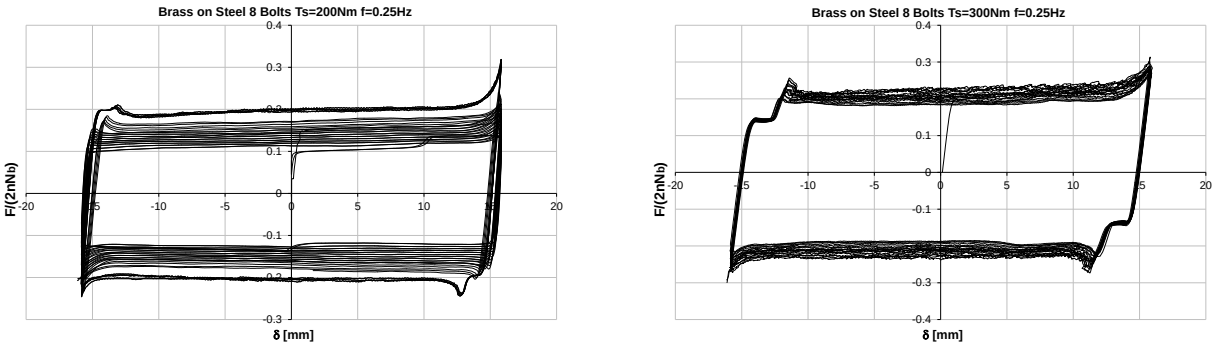

Cycles 1-30 (Ts=200Nm) *Cycles 31-50 (Ts=300Nm)*

Fig. 5. Friction Coefficient – Displacement curves for brass-steel interface

The results of the two tests, reported in Fig. 5, highlight that the behavior of the steel-brass interface is characterized by a first sliding force quite lower compared to the steel-steel interface but, nevertheless, as the number of cycles increases the sliding force also increases exhibiting an hardening behavior. This phenomenon has already been shown in case of steel-steel interface, but in

case of steel-brass interface is less marked. This is probably due to the higher hardness of brass that slows the abrasion process of the surfaces in contact (Fig. 4).

The last metallic pad tested in this work is composed by an 8 mm steel plate on which a layer of aluminum, with a thickness of 300 μm, is thermally sprayed. The spraying is obtained by an industrial procedure similar to the metal arc welding which allows to obtain a coating made of a thin layer of aluminum. This technique, which is usually applied to steel in order to get a cathodic protection, can be effectively applied also for obtaining a plate characterized by frictional properties similar to that of the aluminum, maintaining a low cost as far as only a thin layer of aluminum is sprayed on steel. Three loading sequences have been applied to this friction pad according to the protocol reported in Table 1. The results of the experimental tests for the three considered values of the applied tightening torque are reported in in terms of μ–δ curves.

The results of the sliding tests outline that the response of the sprayed aluminum pad is more stable and with an higher initial value of the friction coefficient compared to the other metallic interfaces. The behavior exhibited by this material under cyclic loads, differently from brass and steel, provides only a slight degradation without initial hardening. In addition, it is easy to recognize from the results of the sliding tests that, in case of sprayed aluminum, there is not a significant difference between the static and dynamic value of the friction coefficient. Nevertheless, the test results also point out that the friction coefficient of sprayed aluminum is significantly influenced by the bolts preloading level. In fact, the sliding force decreases as far as the value of the tightening torque increases.

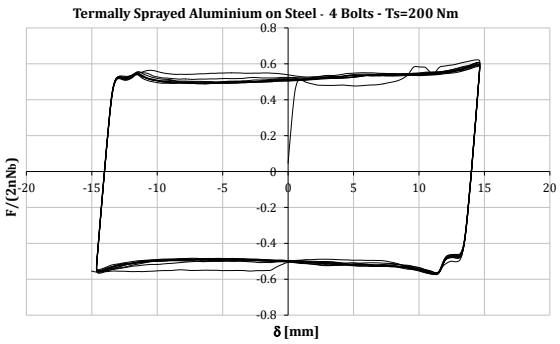

Cycles 1-10 (Ts=200Nm)

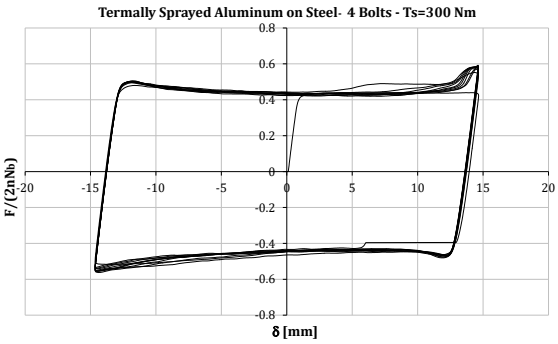

Cycles 11-20 (Ts=300Nm)

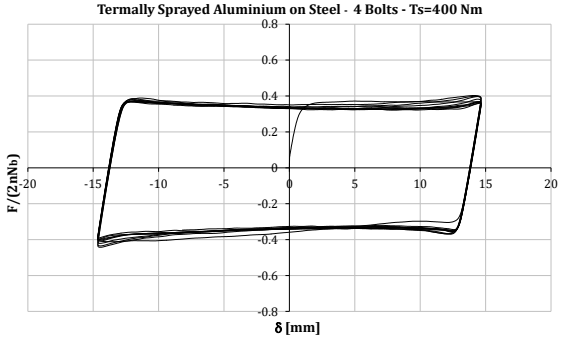

Cycles 21-30 (Ts=400Nm)

Fig. 6. Friction Coefficient – Displacement curves for Sprayed aluminum-steel interface

Starting from the experimental results of the sliding tests, the variation law of the coefficient of friction has been determined for the three considered metallic friction interfaces (Fig. 7). From Fig. 7 it is possible to note that the static coefficient of friction is equal to 0.173 for steel and equal to 0.097 for brass, while in case of sprayed aluminum it varies depending on the bolt pre-loading level in the range 0.37-0.51. It is worth to note that the application of Eq.(4) deriving from the classical Bowden and Tabor theory is able to provide a quite accurate estimate of the static friction coefficient both for brass and steel. In fact, taking into account that the nominal yield strength of S275JR steel grade is equal to 275 MPa and the Vickers hardness is equal to HV 95 (95 kg/mm2) (Kelly & Sha, 1999) and the mechanical properties of brass reported in Table 2**,** the following expressions can be written:

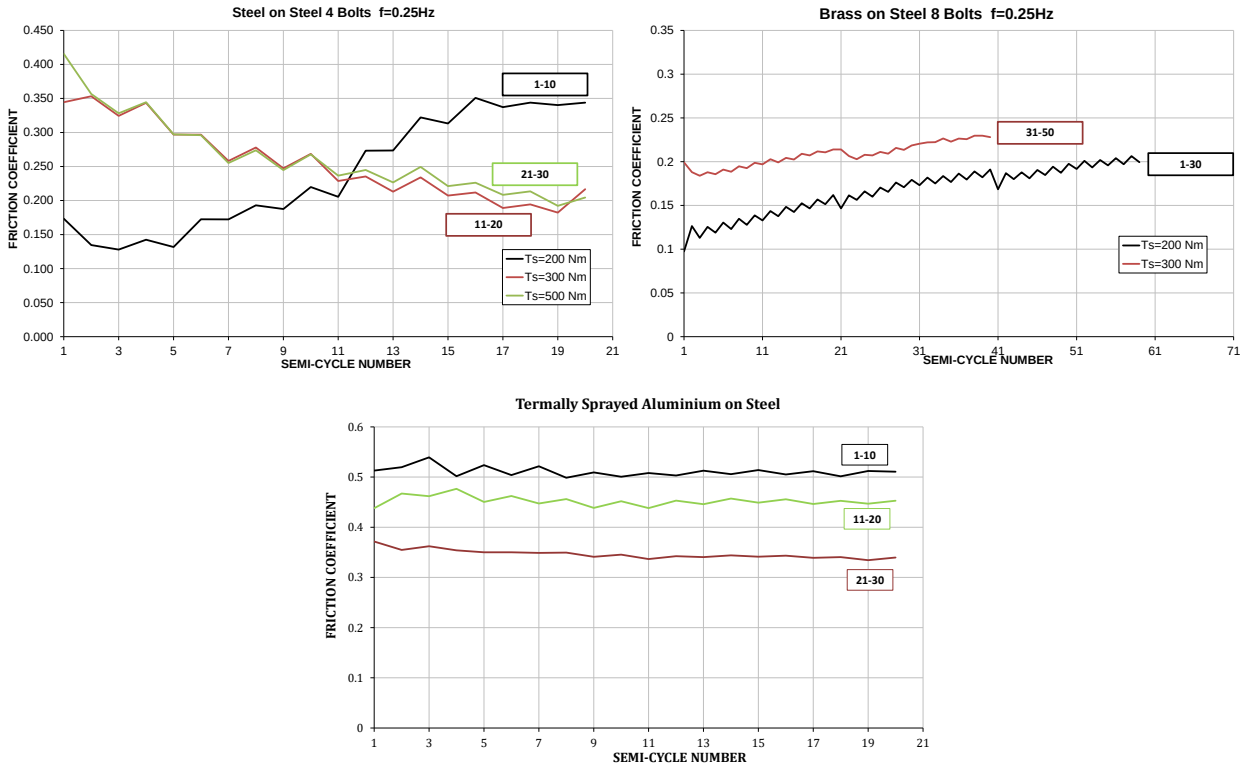

Fig. 7. Friction coefficient for metallic interfaces

$$\boldsymbol{Steel-Steel} \quad \mu = \frac{s_0}{\sigma_0} = \frac{275/\sqrt{3}}{95 \times 9.81} = 0.170 \tag{10}$$

$$\boldsymbol{Brass-Steel} \quad \mu = \frac{s_0}{\sigma_0} = \frac{140}{\sqrt{3} \times 116 \times 9.81} = 0.071 \tag{11}$$

which lead to results very close to the coefficients of static friction experimentally found.

In case of steel-steel interface, during the first loading sequence, after few cycles, the friction coefficient increases up to a value equal to 0.344. During the second and third loading sequence the coefficient initially assumes a value approximately equal to 0.35-0.40 and then quickly decreases up to a value of about 0.20 following approximately the same degradation law. This result reveals that the degradation rate of the friction coefficient of steel does not depend on the pressure acting on the interface. Conversely, in case of brass, the friction coefficient monotonically increases reaching at the end of the second loading sequence a value approximately equal to 0.23. Finally, in case of sprayed aluminum, it is possible to observe from Fig. 7 that there is not a significant difference between the initial and final value of the friction coefficient which decreases always less than 10%.

Starting from the results reported in Fig. 7, it is also possible to carry out some considerations about the relationship existing between the steady state value of the friction coefficient and the pressure applied to the frictional interface. In particular, the pressure applied on the interface can be estimated by assuming that the normal force spreads from the bolt head through the plate thickness with a slope equal to 45° (Faella et al., 1998b):

$$p = \frac{4N_b}{\pi\left(2t_p + d_{bh}\right)^2} \tag{12}$$

where t_p is the outer plate thickness and d_{bh} is the diameter of the bolt head.

In Fig. 8 the dynamic coefficient of friction versus the pressure acting at the interface is depicted for steel and sprayed aluminum plates.

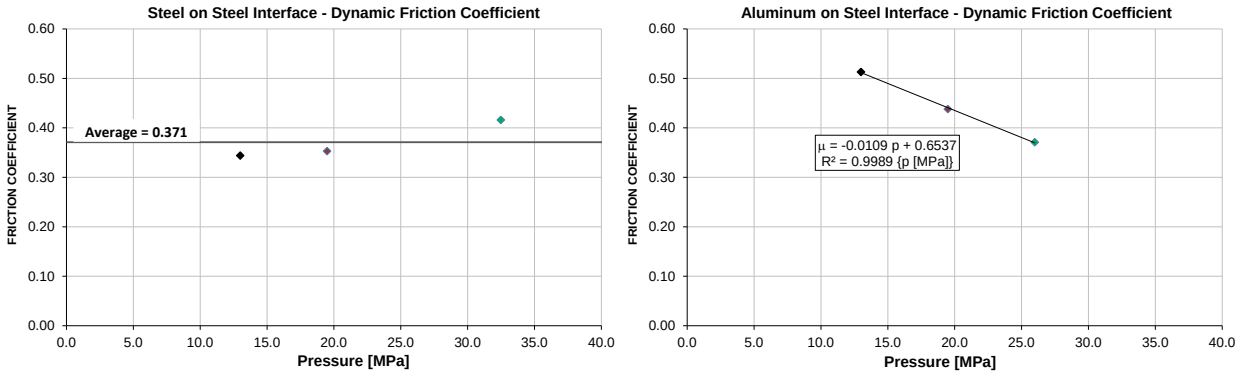

Fig. 8. Dynamic Friction coefficient versus interface pressure

As expected, there is not a significant dependence between the two parameters in case of steel, while in case of aluminum a significant decrease of the friction coefficient arises for increasing values of the applied pressure. In particular, in this last case (Fig. 8), a regression analysis of the friction coefficient versus applied interface pressure, based on experimental results, is proposed (R^2=0.99).

Furthermore, in Fig. 9 the ratio between the force of i-th semicycle and that of the initial one is reported. The results confirm that, in case of steel, the second and third loading sequence exhibit a rapid decrease of strength. In fact, 20% of strength degradation is reached after 7 and 5 cycles, respectively. Dealing with brass, the ratio between the slip force of the i-th semicycle and that of the initial one shows the hardening behavior, outlining a substantial difference between the first and the second loading sequence. In fact the slope of the curve corresponding to the second loading sequence is negligible revealing that, after the initial hardening phase, the friction coefficient stabilize. Concerning sprayed aluminum, it is easy to recognize from the results reported in Fig. 9 that, differently from the initial value of the friction coefficient, there is not a significant dependence between the force degradation law and the value of the pressure applied on the frictional interface.

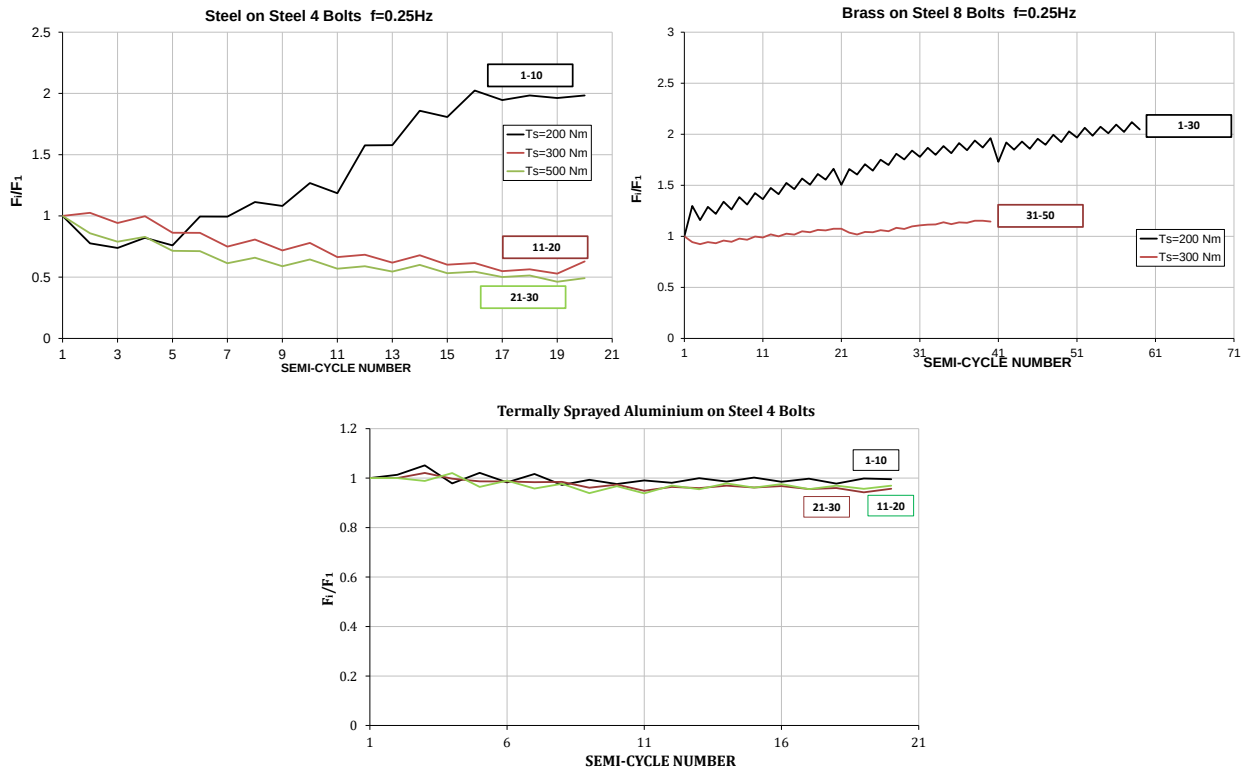

Fig. 9. Ratio between the force of the i-th semicycle and the initial one

Rubber Materials

In the following, the results of three different types of rubber materials sliding on steel are presented. The first material described in this paper is a non-asbestos friction material used for standard braking application, which will be called in the following M0. The material is a blend of mineral and organic fibers aggregated by means of phenolic resin. In particular, material M0 has been tested by the producer, for mechanical engineering application, following the standard test SAE J661. In this test, which is mainly devoted to the investigation of the friction coefficient of

pads subjected to loads simulating braking conditions, the friction pad is located into a machine in contact with a 11-inch drum rotating at speed of 417 rpm. The brake pad is clamped with a constant pressure equal to about 1 MPa. On the base of this testing condition the typical value of the friction coefficient suggested by the producer is 0.51.

The results of the four tests carried out according to the protocol reported in Table 1 are delivered in Fig. 10 showing that M0-steel interface provides a very stable behavior with a significant amount of energy dissipation and low strength degradation. In particular, during the first and second step of loading (1^{th}-40^{th} cycle) the specimen exhibited a very regular behavior, with negligible strength degradation. In addition, a negligible difference between the static and dynamic friction coefficient has been observed. In the third and fourth loading sequence, i.e. from the 41^{th} to 60^{th} cycle the response of the interface is characterized by strength degradation due to the higher initial pressure acting on the interface. In all the four tests the behavior has been of the softening type. Therefore the force reached during the first cycle is always the greatest of the loading history. This behavior is mainly due to the wearing of material during the sliding motion leading to the loss of bolt preloading (Fig. 10).

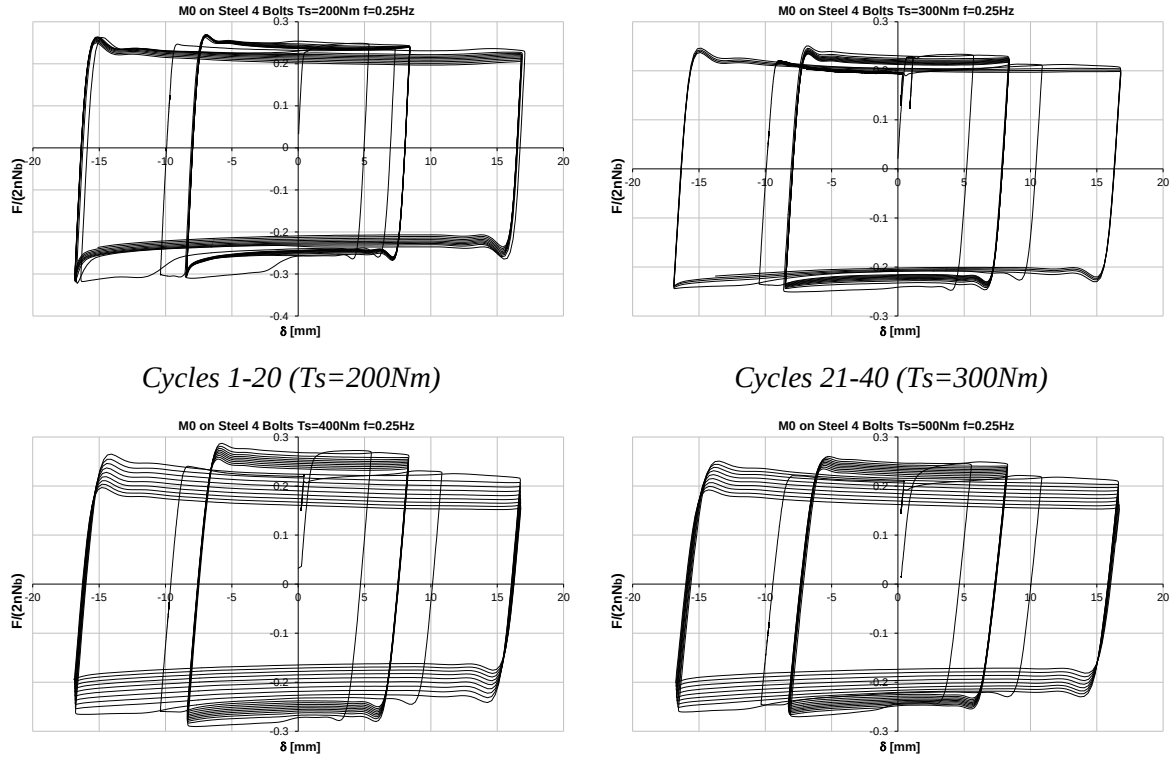

Cycles 1-20 (Ts=200Nm) *Cycles 21-40 (Ts=300Nm)*

Cycles 41-60 (Ts=400 Nm) *Cycles 61-80 (Ts=500 Nm)*

Fig. 10. Friction Coefficient – Displacement curves for M0-steel interface

Afterwards, also another friction material developed by an Italian Factory for applications to electric motors has been tested (Material M1). It is a black flexible material with metallic particles and it is composed by blending mineral, steel and synthetic fiber, nitrilic rubbers and phenolic resin. In this case, the average value of the friction coefficient determined on the base of SAE J661 test proposed by the producer is equal to 0.43. The obtained results, depicted in Fig. 11 in terms of $\mu-\delta$ curves, highlight the peculiarities of the response of material M1 which is characterized by a quite stable behavior for low values of the tightening torque but, for values higher than 300 Nm, it exhibits significant stiffness and strength degradation. This poor performance is due to the low tensile resistance of the friction material which, after the 4th loading sequence, collapsed with the development of a crack at the transversal section weakened by the holes, leading to the complete fracture of the friction pad. Like in case of material M0, also for this rubber based material the softening of the friction resistance occurred in all the four loading sequences.

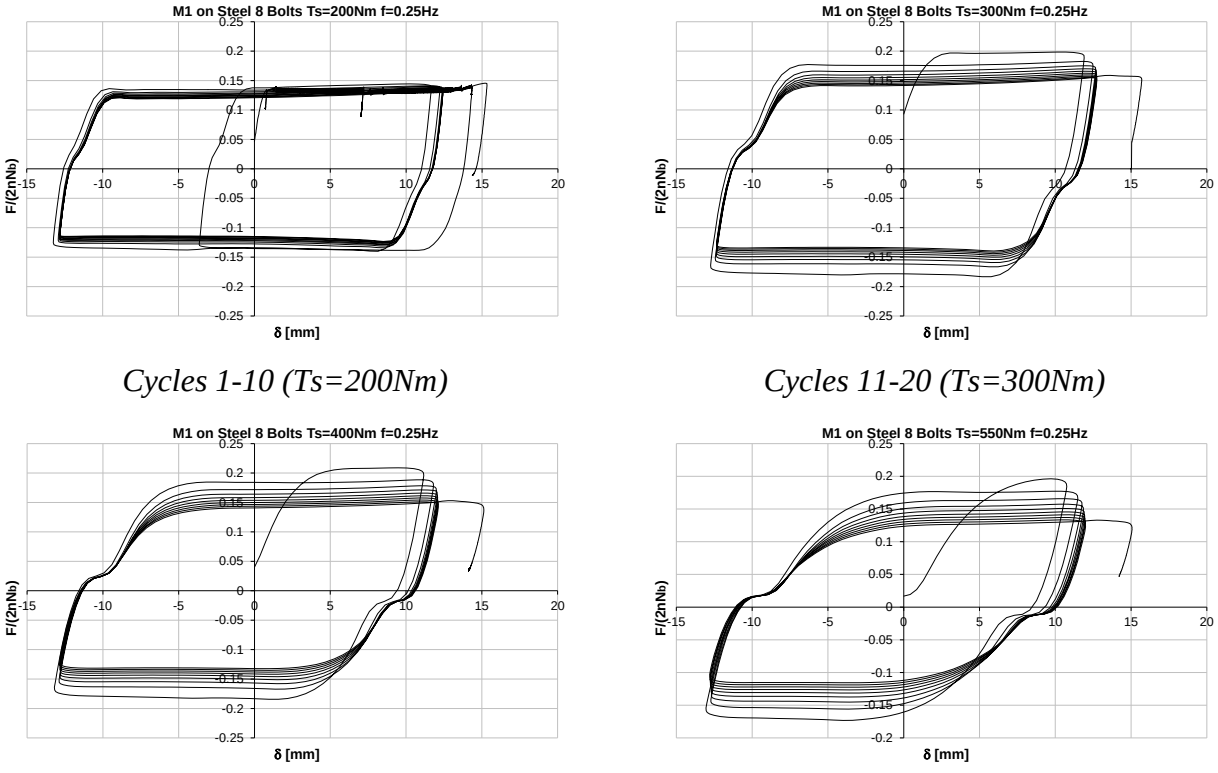

Cycles 1-10 (Ts=200Nm) *Cycles 11-20 (Ts=300Nm)*

Cycles 21-30 (Ts=400 Nm) *Cycles 31-40 (Ts=500 Nm)*

Fig. 11. Friction Coefficient – Displacement curves for M1-steel interface

Therefore, also in this case there is a significant influence of the material wearing (Fig. 12) on the developed cyclic sliding force. In addition, the results obtained for material M1 have not pointed out a substantial difference between static and dynamic friction coefficient.

The last rubber material tested is a friction material developed by an Italian Factory for applications where low wearing is necessary (Material M2). In fact, the material is characterized by a very high ShoreD hardness and, therefore by a good resistance to abrasion. Similarly to material M1, it is a black hard and stiff material composed by a blending mineral and synthetic fiber, nitrilic rubbers and phenolic resin.

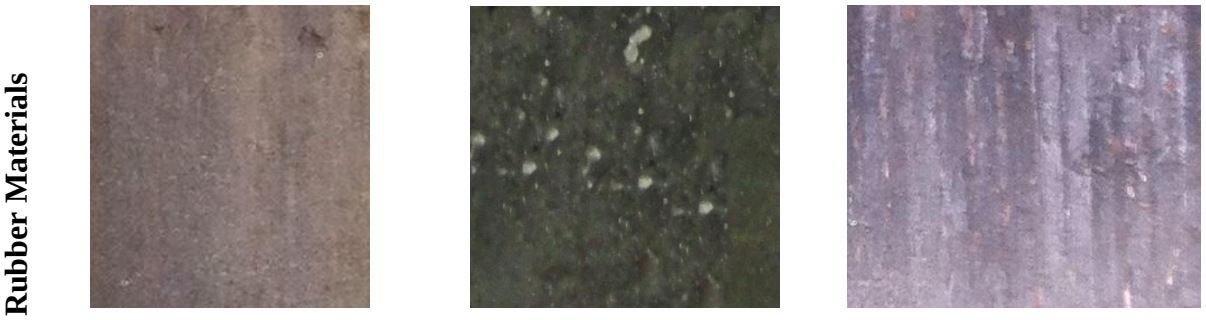

Material M0 *Material M1* *Material M2*

Fig. 12. Texture of the Materials after the test

The mean value of the friction coefficient declared by the producer for contact pressure equal to 1 MPa is equal to 0.36. The results delivered in Fig. 13 point out that M2-steel interface provides a response characterized by three main phases. In the first loading sequence, i.e. cycles from 1th to 10th, during the first cycle after the linear branch a peak corresponding to the static friction is reached and then the interface slides showing a slight hardening behavior. In the subsequent cycles, increasing values of the sliding force are exhibited. In the second test, namely cycles from 11th to 20th, the behavior is very stable and the same value of the sliding force is reached in all the cycles. Only in the third loading sequence a softening behavior is exhibited where the slip resistance progressively reduces as far as the number of cycles increases.

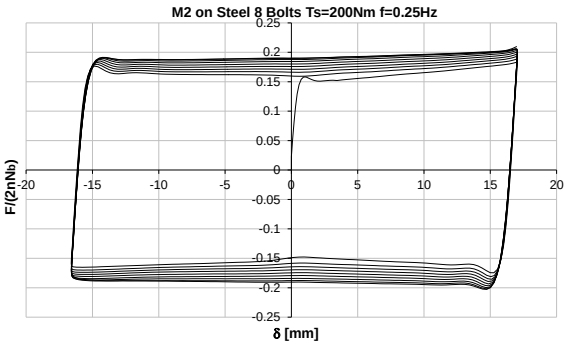

Cycles 1-10 (Ts=200Nm)

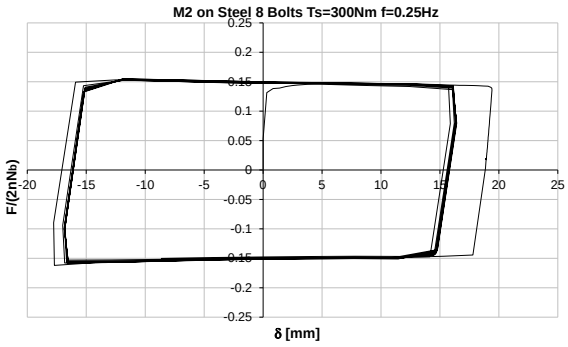

Cycles 11-20 (Ts=300Nm)

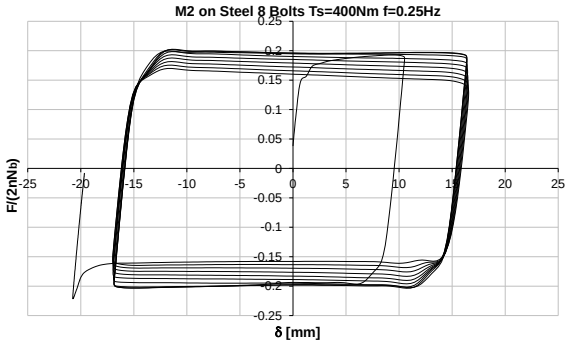

Cycles 21-30 (Ts=400 Nm)

Fig. 13. Friction Coefficient – Displacement curves for M2-steel interface

Similarly to the case of metallic materials, also for rubber interfaces the values of the friction coefficients have been evaluated by means of Eq.(8)-(9) (Fig. 14). This figure points out the different behaviors exhibited by the three materials. In case of material M0, in all the loading sequences the friction coefficient starts from a value of about 0.25 and decreases as far as the number of cycle increases. It is useful to observe that, in the considered tests, a constant frequency has been chosen and, therefore, the change of amplitude at each loading step results in a change of the sliding velocity from 7.5 mm/s to 15 mm/s. Consequently, it can be also observed that the friction coefficient of material M0 is not significantly affected by the sliding velocity.

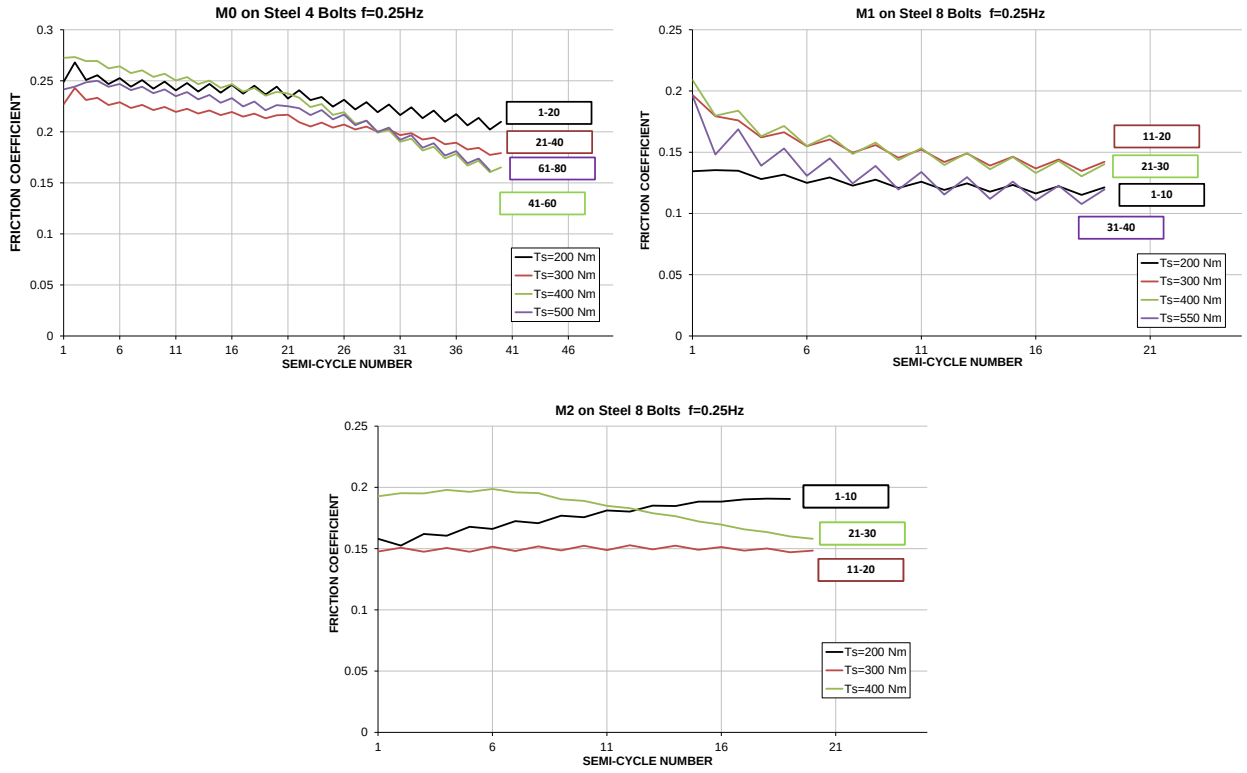

Fig. 14. Friction coefficient for rubber interfaces

The behavior of material M1 is similar to that of material M0 in terms of degradation. In fact, the friction coefficient starts from a value of about 0.2 and successively quickly decreases. In the first loading sequence, corresponding to the minimum tightening torque, the lowest friction coefficient has been obtained. Probably this anomalous result is due to an imperfect application of the tightening torque. Conversely, in case of material M2, a different behavior has been observed. In fact, due to the initially hardening behavior, the experimental values of the static and dynamic friction coefficients are not coincident, being the static friction coefficient equal to 0.158 while the dynamic friction coefficient has an average value equal to 0.178. In addition, in contrast with the outcomes of tests on M0 and M1 friction materials, during the first loading sequence, starting from a static friction coefficient equal to 0.158, increasing values have been observed. In the second loading sequence an almost constant friction resistance has been obtained and, finally, in the third loading cycle sequence a softening behavior has been pointed out.

In order to provide a tool for estimating the kinematic friction coefficient of the tested rubber materials, as for metallic interfaces, the dependence between the friction coefficient and the interface pressure has been examined. It is worth to note that the average value of the friction coefficients obtained in the sliding tests on the three materials by varying the interface pressure in the range 13-33 MPa is considerably lower than the values given by the producer, equal to 0.51-0.43-0.36 for materials M0-M1-M2, respectively, which are defined in correspondence of an interface pressure equal to 1 MPa. This behavior can be easily explained considering the friction laws usually adopted in technical literature to represent the dependence between the friction coefficient and the normal pressure for rubber based materials. In fact, Eqs.(5)-(7) show that in case of rubbers, usually the coefficient of friction decreases as far as the interface pressure increases and tends to become constant at very high pressures. The range of interface pressure values 13-33 MPa investigated in this work are aimed at structural engineering applications, while SAE J661 standard test is, in truth, conceived for automotive applications, where the interface pressure is significantly lower. Therefore, in Fig. 15, the law proposed by (Ratner & Sokolskaya, 1956) is used to carry out a regression analysis by considering both the point given by the producer and the points found in this testing program. In any case, it is worth to say that for structural applications a constant value of the friction coefficient can be assumed with sufficient approximation.

Moreover, in Fig. 16 the ratio between the slip forces of the i-th semicycle and that of the initial one are reported. For material M0 the results highlight that for bolt torques greater than 300 Nm the force decreases much more quickly. Conversely, in case of material M1, due to the low resistance to abrasion, the results show that in all the considered cases a very quick strength degradation is obtained. Therefore, material M1 cannot be considered adequate for structural applications with

high values of the interface pressure. Dealing with material M2, the results show, as expected, a high resistance to abrasion leading to a low strength degradation which, in the considered cases, is always less than the 20%.

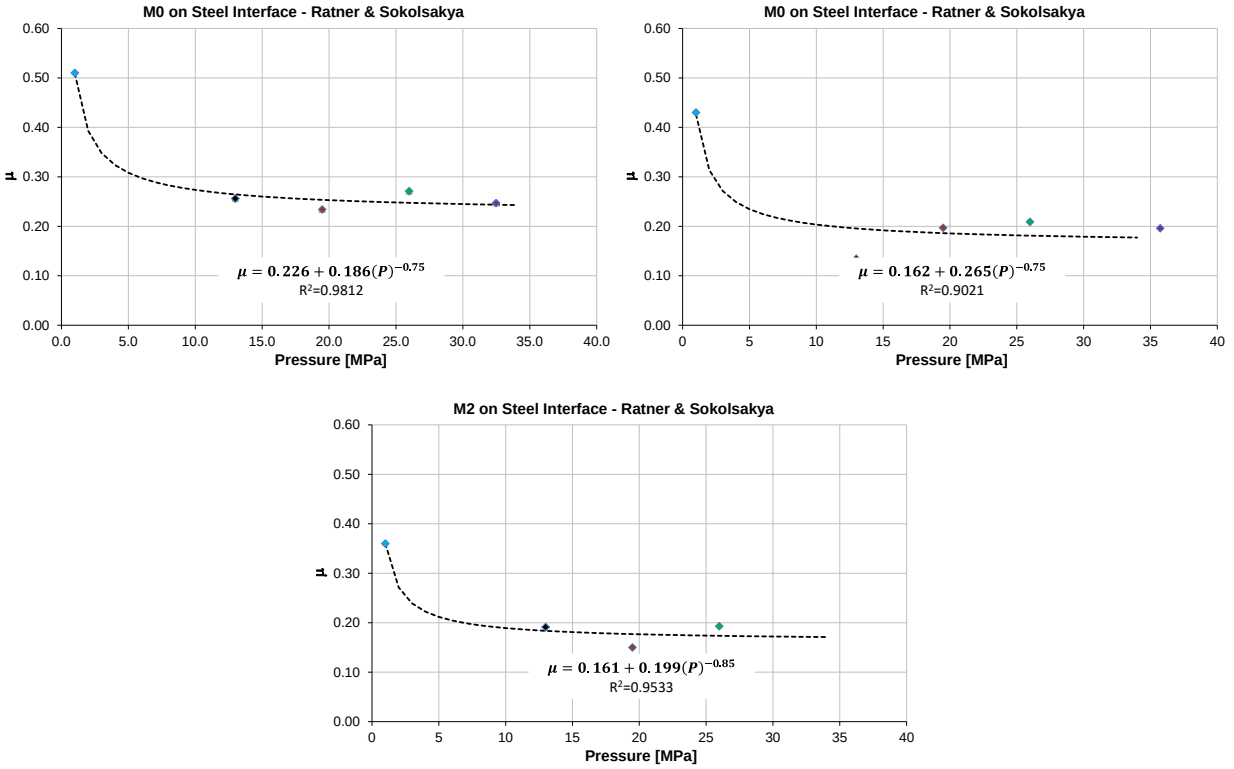

Fig. 15. Dynamic Friction coefficient versus interface pressure

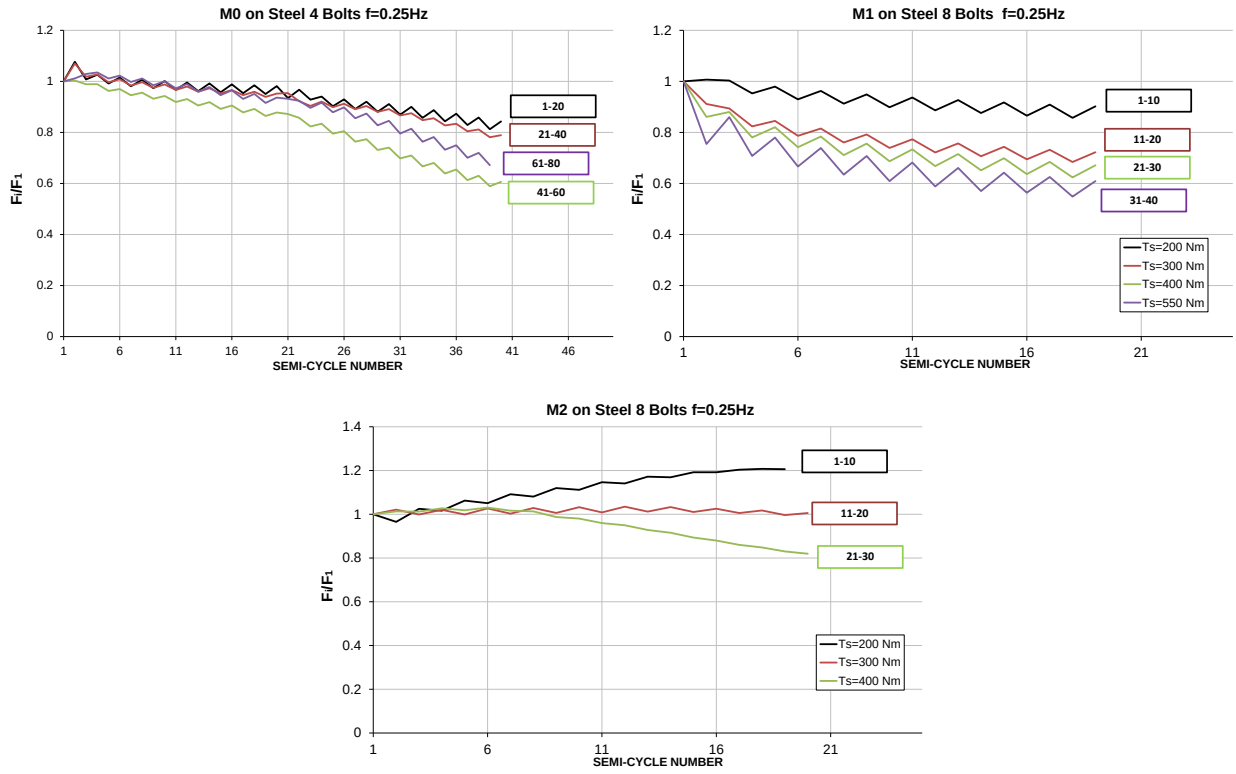

Fig. 16. Ratio between the force of the i-th semicycle and the initial one

EXPERIMENTAL TESTS WITH DISC SPRINGS

The application of the clamping force in a friction device by means of preloaded high strength bolts requires two design issues of paramount importance to be considered: the keeping of the preloading force during the lifetime of the friction damper and the reduction of the loss of the preloading level during the sliding motion. In fact, during the motion, the sliding force can decrease due to the wearing of the friction material. In order to keep the preloading force during lifetime and to reduce drawbacks coming from material consumption, the use of disc spring washers can be suggested.

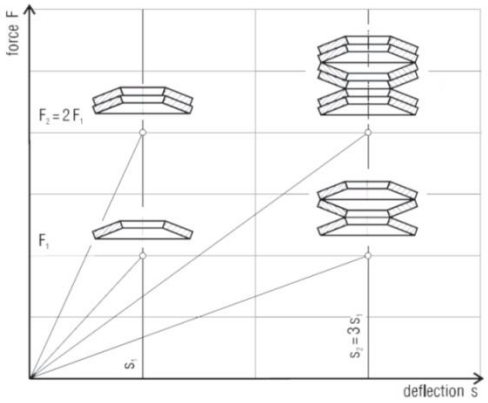

Fig. 17 Possible Combination of Disc Springs (Schnorr, 2003)

Such a type of washer is an high resistance cone shaped annular steel disc spring which flattens when compressed and returns to its original shape if compression loading is released. In this way, if the bolt had to lose the preloading level due to the wearing of the friction material, the disc spring would restore the force by keeping the bolt shaft in tension. The particular shape of cone washers allows single springs to be combined in different ways depending on the desired load-displacement curve. In particular, they can be stacked (Fig. 17):

- in the same direction (parallel stacking): in this way a stiffer spring is obtained;
- in alternating direction (series stacking): in this way a more flexible spring is obtained;
- spring stack of parallel sets in series: in this way a proper combination of washers located in parallel and in series allow to obtain a predetermined value of the stiffness.

In order to evaluate the effect of disc springs on the variation of the sliding force under cyclic loading conditions, further tests have been carried out on material M0 and material M2 by applying a couple of disc springs stacked in series under the bolt nut. In particular, cone washers with internal diameter, external diameter, height and thickness equal to 21, 45, 6.4 and 5 mm, respectively, have been used. Such a kind of washer completely flattens under a load equal to 130

kN. In order to compare the cyclic behavior the same loading protocol has been adopted. Conversely, material M1 has not been tested again because of its poor behavior with circular flat washers. In particular the following additional tests have been carried out:

- M0-Steel Interface: Bolts torque = 200 Nm, 10 cycles with amplitude of 7.5 mm and 10 cycles with amplitude of 15 mm;
- M2-Steel Interface: Bolts torque = 200 Nm, 10 cycles with amplitude equal to 15 mm.

Regarding friction material M0, the new specimen exhibited a behavior similar to that obtained in the test with circular flat washers, but lower degradation was obtained (Fig. 18).

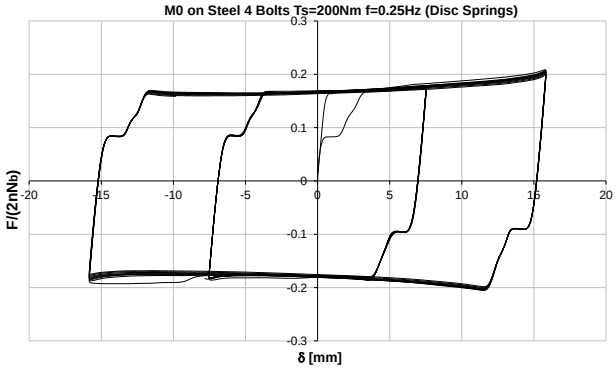

Fig. 18. M0 on Steel interface with Disc Springs - Force-Displacement curve

The comparison between the two tests in terms of friction coefficient shows that in the test with disc springs a lower value of the initial friction coefficient has been obtained, because the friction pad has not been substituted after the test with flat washers. Conversely a more stable behavior in terms of strength degradation and energy dissipation capacity has been exhibited (Fig. 19).

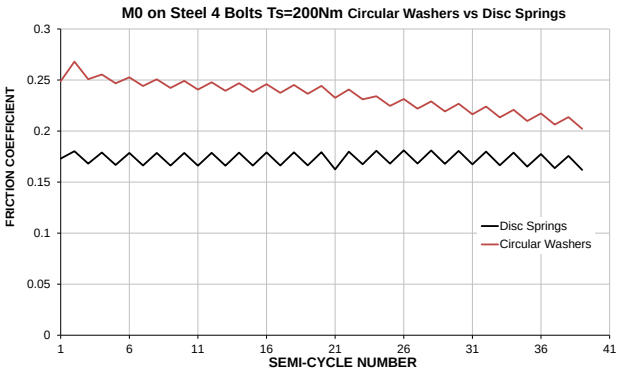

Friction coefficient versus cycles

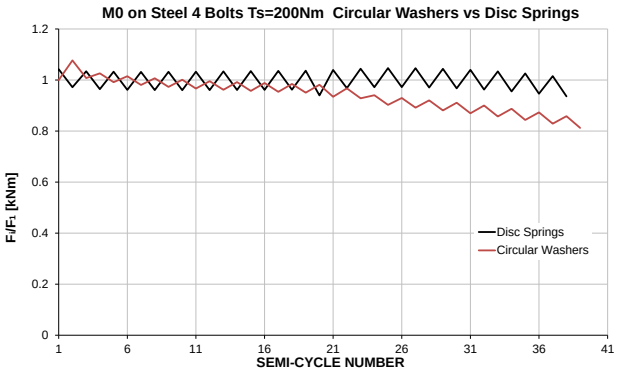

Ratio between i-th sliding force and initial one

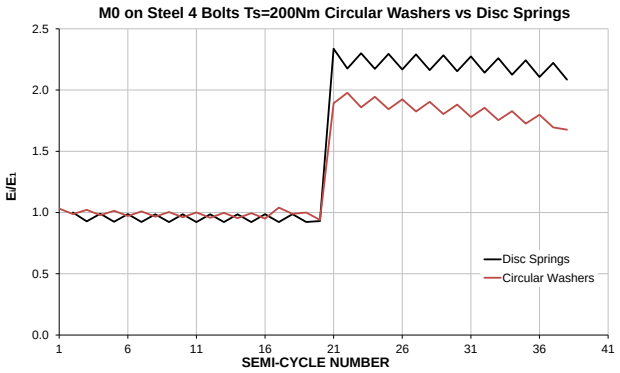

Dissipated energy: ratio between i-th cycle first cycle

Fig. 19. M0 on Steel interface - Circular Washers vs Disc Springs

Regarding friction material M2 (Fig. 20), starting from a force of about 120 kN, after the first sliding, the new specimen exhibited a slightly hardening behavior.

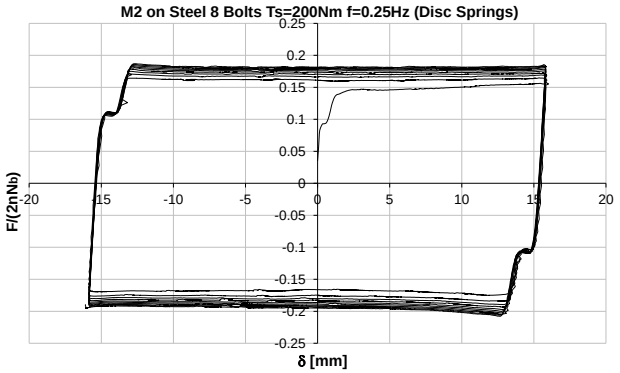

Fig. 20. M2 on Steel interface with Disc Springs - Force-Displacement curve

The comparison with the test with flat washers points out that the friction coefficient is almost unaffected, it starts from a static value of about 0.15 and then increases to about 0.19. Similarly, in both tests, there is an increase of strength and energy dissipation capacity, with respect to the first cycle, of about the 20%.

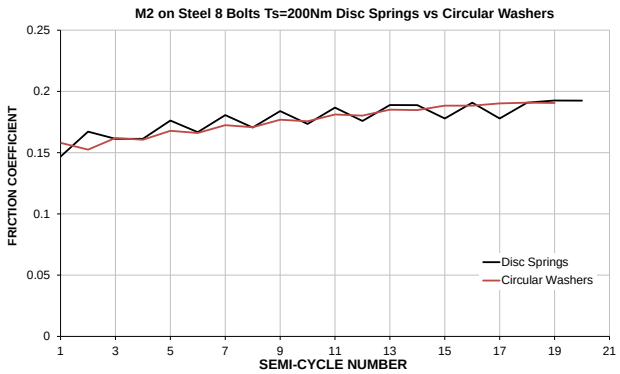

Friction coefficient versus cycles

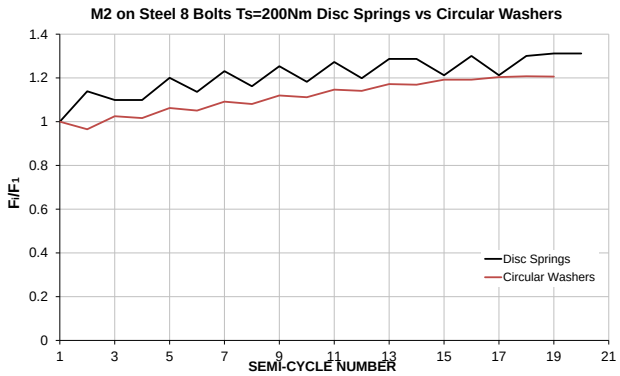

Ratio between i-th sliding force and initial one

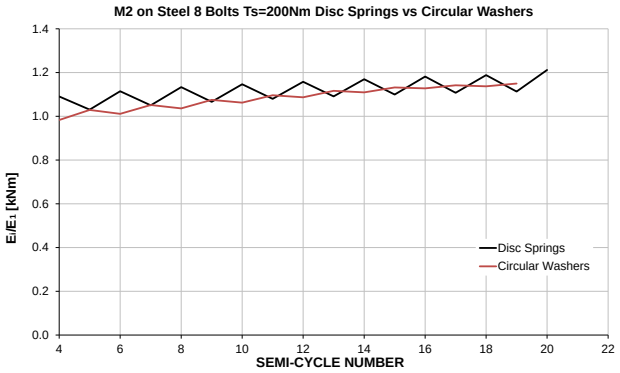

Dissipated energy: ratio between i-th cycle first cycle

Fig. 21. M2 on Steel interface - Circular Washers vs Disc Springs

Therefore, on the base of the obtained results, it seems that the application of disc springs provides only a slight improvement of the response under cyclic loads. Nevertheless, as aforementioned, the application of disc springs in practice can be useful for keeping the preloading level during the lifetime of the dissipative device. In fact, as already demonstrated by (Heistermann, 2011), tightened bolts are usually affected by a short term relaxation, which occurs within the first twelve hours after joint assembly, and a long term relaxation, which usually continue asymptotically during the time. Furthermore, when groups of bolts are tightened, there is also a loss of pretension due to a mutual effect, i.e. after any bolt tightening the bolts previously tightened experience a loss of pretension. All these effects can be reduced by means of annular cone disc springs.

MATHEMATICAL MODELING OF FRICTION MATERIALS

In order to provide a practical tool to be employed in the design and modeling of the response of friction pads to be applied to supplemental damping devices, a mathematical model able to predict the cyclic behavior of the friction materials investigated in this paper has been carried out. Aiming to the use of such materials in friction dampers for seismic design applications, the requirements to be satisfied regard the coefficient of friction which, under cyclic loading conditions, should be as high as possible in order to reduce the size of the damping devices and, in addition, the stability of the cyclic behavior. Therefore, on the basis of the experimental results previously presented, in the following, only three interfaces have been selected: steel-steel, sprayed aluminum-steel and material M0-steel, i.e. those characterized by the higher values of the friction coefficient and by hardening or slightly softening response.

Dealing with steel-steel interface, as aforesaid, its behavior is characterized by two different phases. In a first phase, due to the progressive ploughing of the surfaces in contact, the friction coefficient quickly increases reaching a constant value, which is maintained before the achievement of a

softening phase due to the material wearing and the partial loss of the bolt preloading force. In this phase, the friction coefficient begins to decay with a law which, as pointed out by testing results, is not dependent on the force applied to the interface.

Therefore, the modeling of the hardening/softening rules of the steel-steel interface can be carried out starting from the test results, by reporting the values of the friction coefficient versus a parameter able to represent the progressive wearing and degradation of the material. In this work, the cumulated value of the energy dissipated is chosen as reference parameter. The result of the analysis is reported in Fig. 22 where the values of the kinematic friction coefficient observed at the i-th cycle divided by the initial value of the friction coefficient are reported versus the cumulated energy both for the hardening and for the softening phase.

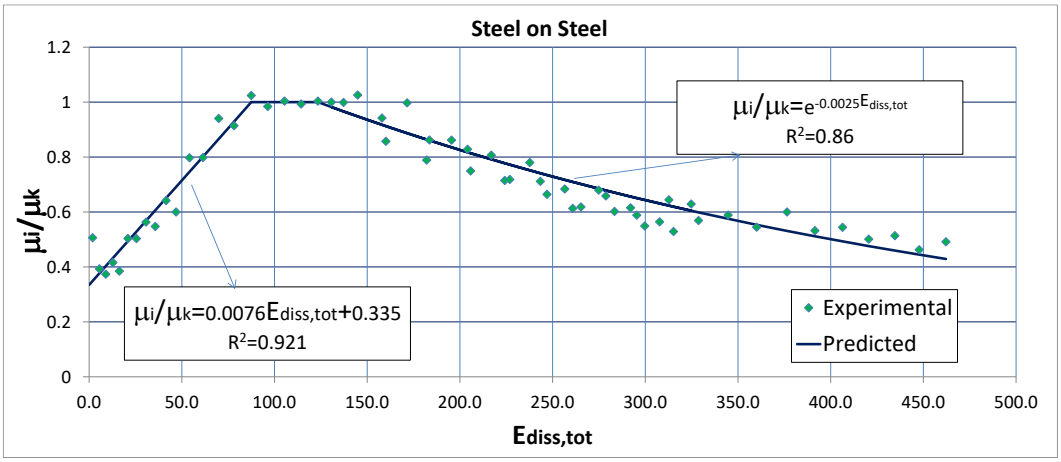

Fig. 22. Regression analysis of experimental data for Steel-Steel Interface

Consistently with the experimental behavior, the model describing the coefficient of friction under cyclic loading conditions is defined by means of the three branches reported in Fig. 22. The first one modeling the hardening phase, characterized by a linear approximation, the second one modeling the steady state phase, assuming a constant value, and the third one describing the softening phase, characterized by an exponential law:

$$\begin{aligned} &\frac{\mu_i}{\mu_k} = 0.0076E_{diss,tot} + 0.335 && 0 < E_{diss,tot} \leq 87\ kNm \ \text{- Hardening phase} \\ &\frac{\mu_i}{\mu_k} = 1 && 87 < E_{diss,tot} \leq 123\ kNm \ \text{- Steady State phase} \\ &\frac{\mu_i}{\mu_k} = e^{-0.0025E_{diss,tot}} && E_{diss,tot} > 123\ kNm \ \text{- Softening phase} \end{aligned} \quad \textbf{(13)}$$

Therefore, starting from the knowledge of the initial value of the dynamic friction coefficient, the cyclic force-displacement response of the steel-steel interface can be predicted by means of Eq.13.

Concerning the modeling of the behavior of the metallic interface made of sprayed aluminum sliding on steel, it can be easily characterized. In fact, as demonstrated by the sliding tests the initial

value of the friction coefficient of this material strongly depends on the interface pressure, but the degradation law does not significantly depend on the pressure applied to the interface. Therefore, in this case, a regression analysis of the data of the three experimental tests has been carried out following the same procedure specified for the steel-steel interface. The obtained results show that the degradation law of the sprayed aluminum-steel interface is described by the following equation which provides a smooth decay law of the friction coefficient:

$$\frac{\mu_i}{\mu_k} = 1 - 0.000328E_{diss,tot} \qquad with\ E_{diss,tot}\ [kNm] \tag{14}$$

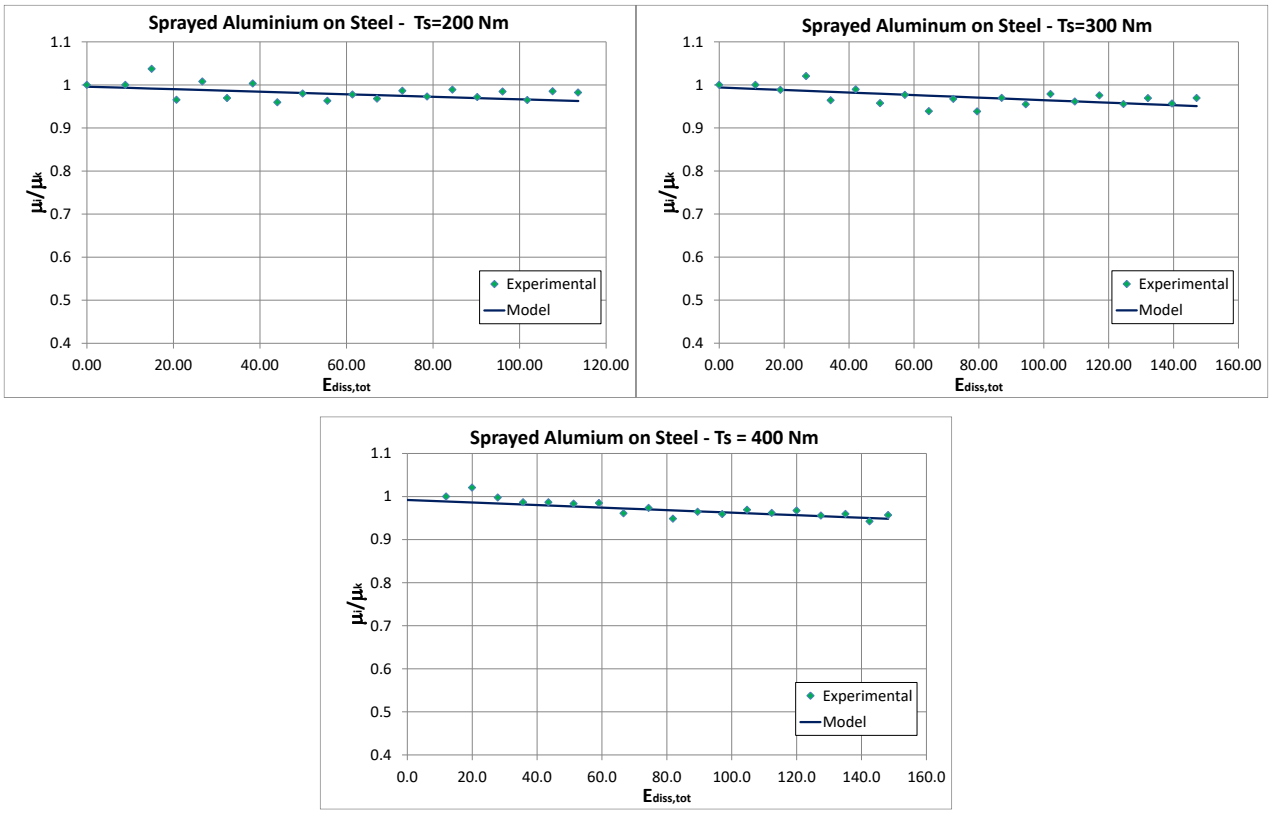

Fig. 23. Regression analysis of experimental data for Sprayed Aluminum-Steel Interface

A model able to describe the degradation law of material M0 has also been defined by exploiting the experimental data coming from the sliding tests. In case of material M0, as aforesaid, the initial value of the friction coefficient always decay providing increasing values of the degradation rate as far as the contact pressures increase. In fact, due to the low value of the ShoreD hardness, material M0 is subjected, under cyclic loadings, to significant wearing which lead to a progressive deterioration of the friction coefficient.

Therefore, starting from the four tests previously reported, a mathematical model able to predict the value of the friction coefficient under cyclic loading histories has been developed. To this scope, a multiple linear regression analysis of the experimental data has been carried by considering two

independent variables: the cumulated value of the energy dissipated and the contact pressure at the interface calculated by means of Eq.12. The following result has been obtained (R^2=0.916):

$$\frac{\mu_i}{\mu_k} = 1 - 0.00216E_{diss,tot} + 0.000284p \qquad with\ E_{diss,tot}\ [kNm] and\ p\ [MPa] \tag{15}$$

The results of the regression analysis are represented in Fig. 24 where the agreement between experimental and predicted values is shown.

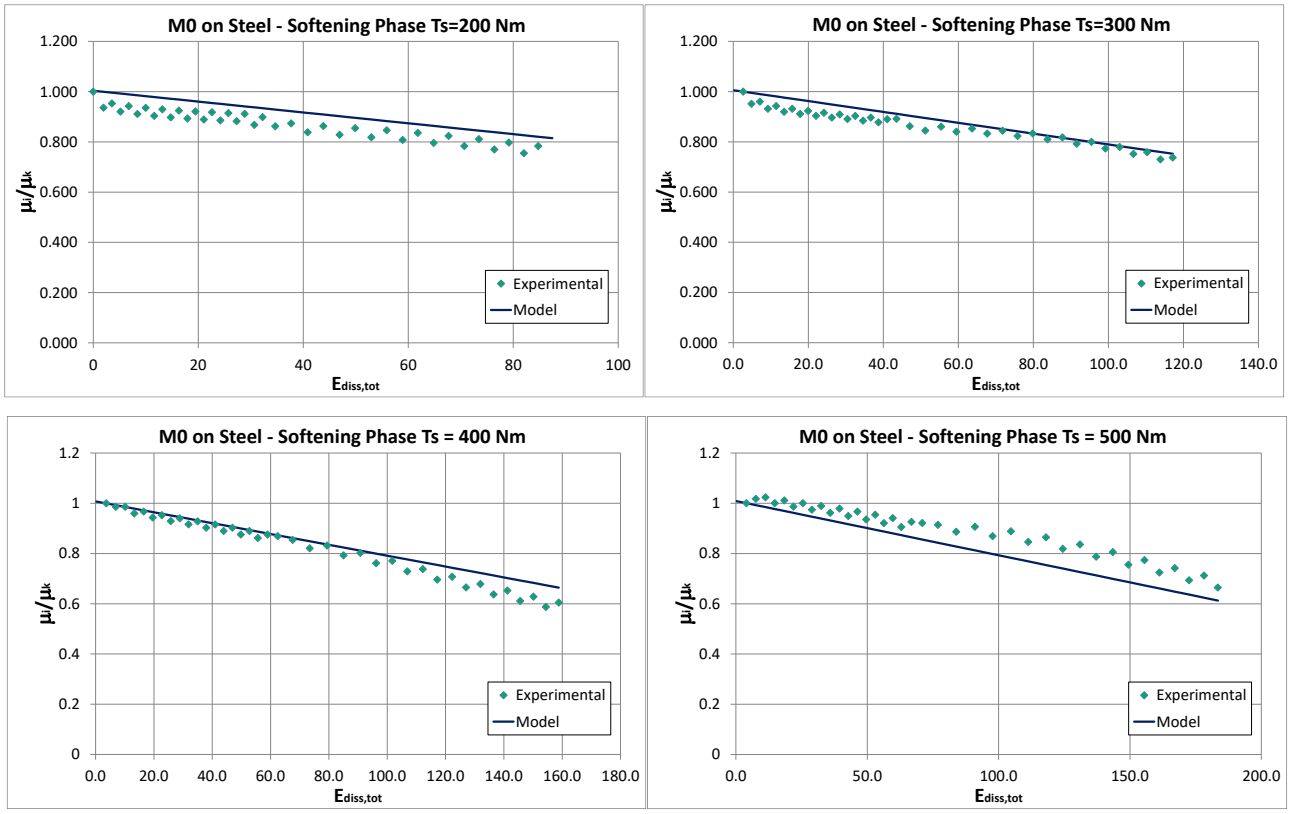

Fig. 24. Regression analysis of experimental data for M0-Steel Interface

In order to show the ability of the proposed models to reproduce the response of the different frictional interfaces, some simulations have been carried out by exploiting the mathematical laws provided by Eqs.13-15 and the values of the friction coefficient defined by equations reported in Figs.8 and 15. In Fig.25 the good agreement between experimental and predicted cyclic response is pointed out.

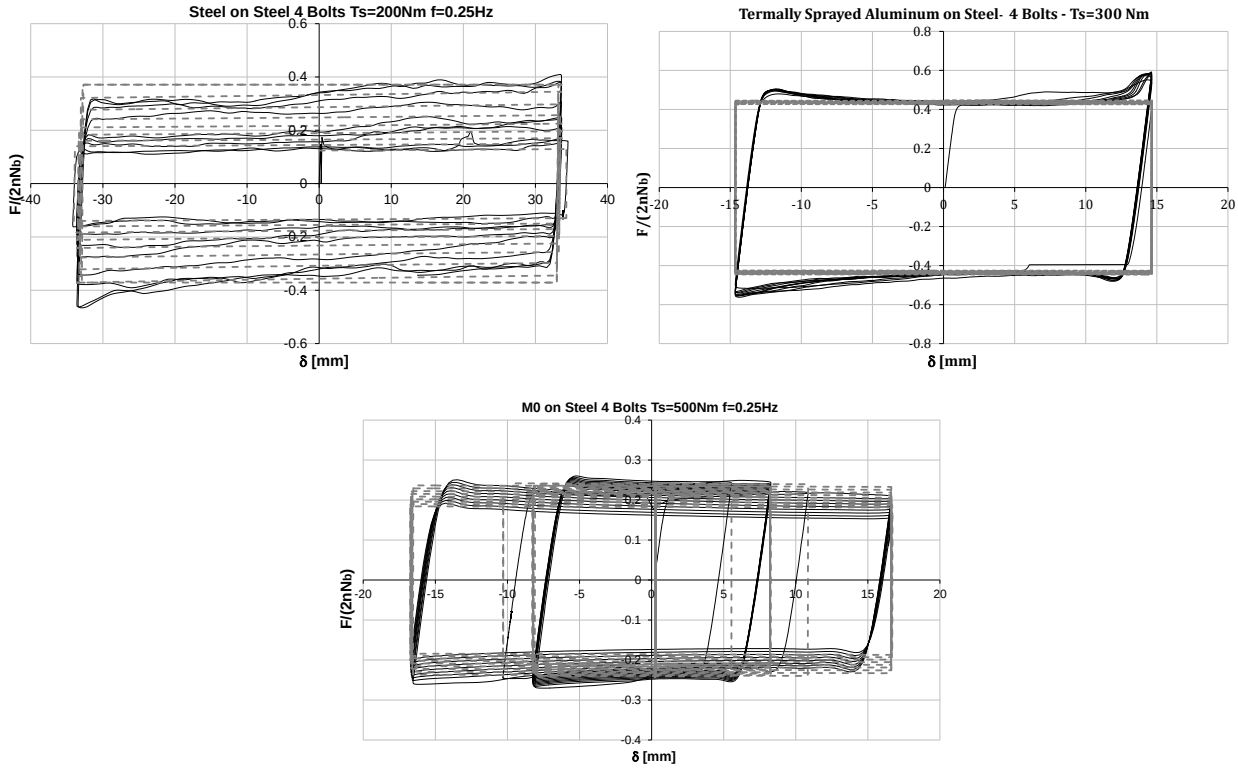

Fig. 25. Application of the proposed mathematical model to some experimental tests

CONCLUSIONS

In this work, an experimental program devoted to the investigation of the frictional properties of six different materials to be used in supplemental damping devices adopting dry friction as source of energy dissipation has been carried out. To this scope a sub-assemblage has been tested by varying the friction interface, the number of preloaded bolts, the tightening torque and the type of washers. In particular, three metallic friction interfaces and three rubber friction pads on steel have been tested.

Regarding metallic friction interfaces, the main results of the experimental program can be summarized as follows:

- Steel on steel interface exhibited high coefficient of friction, but a quite unstable behaviour which is initially characterized by a significantly hardening behaviour and successively by a rapidly softening behaviour;
- Brass on steel interface exhibited a quite low value of the friction coefficient and a stable behaviour characterized by a significant hardening;
- Thermally sprayed aluminum on steel interface exhibited an high value of the friction coefficient and a cyclic response with small degradation.

Concerning rubber friction pads, the following main observations can be made:

- Material M0, which is a rubber based material developed for automotive applications exhibited a very stable behaviour and high energy dissipation capacity also under high values of the preloading level;
- Material M1, which is a rubber based material developed for electrical machines, exhibited pinching behavior, low friction coefficient and a rapidly degrading behavior;
- Material M2, which is a hard rubber based material developed for applications where low wearing is necessary, developed a quite low value of the friction coefficient, but a very stable behavior and high energy dissipation capacity.

The work herein presented is part of a research program aiming to the use of such materials in friction dampers to be adopted within the structural detail of innovative dissipative beam-to-column connections, based on bolted double split tee configuration, for seismic design applications (Latour et al. 2011a). To this scope, an high value of the coefficient of friction is desired in order to reduce the size of the friction damper. In addition, a stable cyclic response is also required. Therefore, on the basis of the experimental results previously presented, three interfaces have been selected seem more appropriate: steel-steel, sprayed aluminum-steel and material M0-steel, i.e. those characterized by the higher values of the friction coefficient and by hardening or slightly softening response. For such interfaces, mathematical models to predict their cyclic response has been developed and compared with experimental test results showing their accuracy. These models are based on an initial value of the friction coefficient and on a law describing its variation as a function of the energy dissipated during the loading history. Depending of the friction interface, the initial value of the friction coefficient can be either dependent on or independent of the applied pressure due to bolt preloading.

Focusing the attention on the three interfaces providing the best results. Even though the initial friction coefficient of thermally sprayed aluminum on steel reduces as far as the applied pressure increases, it can be recognized that it gives rise to the highest value of the initial friction coefficient. In addition, such interface is able to provide quite stable hysteresis loops with only small degradation. Therefore, the authors believe that the use of friction pads made of steel plates with thermally sprayed aluminum can represent a good solution to improve the bending performance and the cyclic response of beam-to-column joints equipped with friction dampers. This issue will constitute the forthcoming development of the planned research activity.

REFERENCES

Aiken, I., Clark, P. & Kelly, J., 1993b. Design and Ultimate-Level Earthquake Tests of a 1/2.5 Scale Base-Isolated Reinforced-Concrete Building. In *Proceedings of ATC-17-1 Seminar on Seismic Isolation, Passive Energy Dissipation and Active Control*. San Francisco.California, 1993b.

Aiken, I., Nims, D., Whittaker, A. & Kelly, J., 1993a. Testing of Passive Energy Dissipation Systems. *Earthquake Spectra*, 9(3).

Alonso, J., 1989. *Mechanical Characteristics of X-Plate Energy Dissipators*. Berkeley: University of California.

Bowden, F. & Tabor, D., 1950. *The Friction and Lubrication of Solids: part I*. Oxford: Oxford University Press.

Bowers, R., Clinton, W. & Zisman, W., 1953. Frictional Behavior of Polyethilene, Polytetrafluorethylene and Halogenated Derivatives. *Lubrication Engineering*, 9, pp.204-09.

Cahis, X., Bozzo, L., Foti, D. & Torres, L., 1997. An Energy Dissipating Device for Seismic Protection of Masonry Walls. In *L'ingegneria Sismica in Italia*. Taormina, Italia, 1997.

CEN, 2005a. *Eurocode 3: Design of steel structures - Part 1-1: General rules and rules for buildings*.

CEN, 2005b. *Eurocode 3: Design of steel structures - Part 1-8: Design of joints*.

Christopoulos, C. & Filiatrault, A., 2006. *Principles of Passive Supplemental Damping and Seismic Isolation*. Pavia: IUSS PRESS.

Constantinou, M., Soong, T. & Dargush, G., 1998. *Passive Energy Dissipation Systems for Structural Design and Retrofit*. State of New York: University at Buffalo.

Faella, C., Piluso , V. & Rizzano, G., 1998b. Experimental Analysis of Bolted connections: snug versus preloaded bolts. *Journal of Structural Engineering*, 124(7), pp.765-74.

Grigorian, C., Yang, T. & Popov, E., 1992. *Slotted Bolted Connection Energy Dissipators*. Berkeley: University of California Earthquake Engineering Research Center.

Halling, J., 1978. *Principles of Tribology*. London: Macmilln Education LTD.

Heistermann, C., 2011. *Behaviour of Pretensioned Bolts in Friction Connections*. Lulea: Lulea University of Technology.

Iannone, F., Latour, M., Piluso, V. & Rizzano, G., 2011. Experimental Analysis of Bolted Steel Beam-to-Column Connections: Component Identification. *Journal of Earthquake Engineering*, 15(2), pp.214-44.

Kelly, J., 1979. Aseismic Base Isolation: A review. In *Proceedings of 2nd U.S. National Conference on Earthquake Engineering*. Stanford, CA, 1979.

Kelly, F. & Sha, W., 1999. A Comparison of the Mechanical Properties of Fire-Resistant and S275 Structural Steels. *Journal of Constructional Steel Research*, 50, pp.223-33.

Kelly, J., Skinner, R. & Heine, A., 1972. Mechanisms of Energy Absorption in Special Devices for Use in Earthquake Resistant Structures. *Bullettin of the New Zealand Society for Earthquake Engineering*, 5(3), pp.63-88.

Kobori, T. et al., 1992. Development of Hysteresis Steel Dampers. In *Earthquake Engineering Tenth World Conference*., 1992.

Latour, M., Piluso, V. & Rizzano, G., 2011a. Experimental analysis of innovative dissipative bolted double split tee beam-to-column connections. *Steel Construction*, 4(2), pp.53-64.

Latour, M., Piluso, V. & Rizzano , G., 2011b. Cyclic Modeling of Bolted Beam-to-Column Connections: Component Approach. *Journal of Earthquake Engineering*, 15(4), pp.537-63.

Latour, M. & Rizzano, G., 2012. Experimental Behavior and Mechanical Modeling of Dissipative T-Stub Connections. *Journal of Structural Engineering*, 138(2), pp.170-82.

Mualla, I. & Belev, B., 2002. Seismic Response of Steel Frames Equiped with a New Friction Damper Device Under Earthquake Excitation. *Engineering Structures*, 24(3), pp.365-71.

Nakashima, M., 1995. Strain-Hardening Behavior of Shear Panels made of Low-yield Steel: Test. *Journal of Structural Engineering ASCE*, 121(12), pp.1742-49.

Pall, A. & Marsh, C., 1981. Response of Friction Damped Braced Frames. *Journal of the Structural Division*, 108(6), pp.1313-23.

Persson, B., 2000. *Sliding Friction*. Berlin: Springer.

Ratner, S. & Sokolskaya, V., 1956. The Influence of the Hardness of Rubber on its Coefficient of Static Friction without Lubrication. *Rubber Chem. Technol.*, 29, pp.829-33.

Rees, B., 1957. Static Friction of Bulk Polymers over a Temerature Range. *Research*, 10, pp.331-38.

Schallamach, A., 1952. The Load Dependance of Rubber Friction. In *Phys Soc.*, 1952.

Schallamach, A., 1958. Friction and Abrasion of Rubber. *Wear*, 1, pp.384-417.

Schnorr, 2003. *Handbook for Disc Springs*. Heilbronn: Adolf Schnorr GmbH.

Shooter, K. & Thomas, R., 1952. Frictional Properties of some Plastics. *Research*, 2, pp.533-39.

Skinner, R., Kelly, J. & Heine, A., 1975. Hysteresis Dampers for Earthquake Resistant Structures. *Earthquake Engineering and Structural Dynamics*, 3, pp.287-96.

Soong, T. & Spencer Jr, B., 2002. Supplemental Energy Dissipation: State-of-the-Art and State-of-the-Practice. *Engineering Structures*, 24, pp.243-59.

Thirion, P., 1948. Les Coefficients d'Adherence du Caoutchouc. *Rubber Chemistry and Technology*, 21, pp.505-15.

Tremblay, R. & Stiemer, S., 1993. Energy Dissipation through Friction Bolted Connections in Concentrically Braced Steel Frames. *ATC 17-1 Seminar on Seismic Isolation*, 2, pp.557-68.

Whittaker, A., Bertero, V., Alonso , J. & Thompson, C., 1989. *UCB/EERC-89/02 Earthquake Simulator Testing of Steel Plate Added Damping and Stiffness Elements*. Berkeley: College of Engineering University of California.

Whittaker, A., Uang, C. & Bertero, V., 1990. *UCB/EERC-88/14 An Experimental Study of the Behavior of Dual Steel Systems*. Berkeley: College of Engineering University of Calfornia.

Zhang, S., 1998. State-of-the art of Polymer Tribology. *Tribology International*, 31, pp.49-60.